Building a feature vector for assessing the gait of persons with multiple sclerosis

Andrew Hynes and Stephen Czarnuch
Memorial University
{ajrh27, sczarnuch}@mun.ca

***Abstract*—We present our recent work towards an automated characterization of gait using non-intrusive motion tracking, with application to the rehabilitation assessment of persons with multiple sclerosis (MS). We used a depth sensing camera to track the walking motion of participants with MS. The system produces multiple predictions for the positions of body parts. We employ a graph theory algorithm to optimally select from these predictions, and estimate the rigid lengths between adjacent body parts. The positions are then treated as point masses in a linear spring system, with each spring having a resting length equal to the estimated length. As the system reaches equilibrium, the positions are forced to conform to these lengths. Using our optimized data, we group the following gait features into a feature vector: stride length and width, walking velocity, and arm swing angle. In future work, we will attempt to distinguish between normal and abnormal gait using these parameters.**

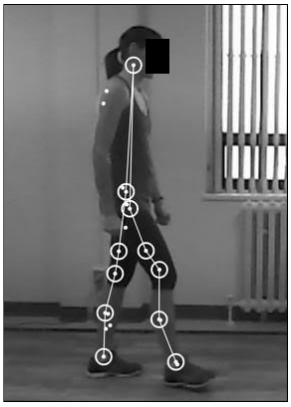

Figure 1. Selection of body part positions from multiple options. The white dots represent all of the optional positions that are available for the image frame. The circled dots are the chosen positions

I. Introduction

Gait analysis has been highlighted as an important tool for clinical therapy [1]–[3], and the assessment of gait has been recently used as a method of monitoring the progression of multiple sclerosis [4], [5]. Unfortunately, gait assessment can require expensive equipment, such as a platform with sensors that record the pressure of a walking person [6]. Analyzing gait using computer vision based techniques could become a more affordable option. Computer vision approaches have previously been used for general gait analysis, using passive markers placed on the tracked body [7], and using depth sensors [8]–[10]. Also, gait analysis with a clinical focus has been performed with a combination of computer vision and wearable sensors [11]. However, there is scarce literature on using depth sensors specifically for the gait analysis of persons with multiple sclerosis, limited to exploratory studies [5].

Our own recent work is this area involved a new method to process the data captured by a single depth sensor tracking the gait of people with MS [12], by selecting accurate body part positions from multiple options using a shortest path algorithm from graph theory [13]. Treating optional part positions as nodes in a graph, edges are placed between the nodes of adjacent body parts. For each body part pair, there is a pre-estimated length between the parts. The current part positions on a given image frame may be spaced closer or further than the estimated length. The weight of the edge between two nodes is based on the difference between the current body length and the estimate true length. By solving the shortest path problem, the sum of the weights is minimized. The nodes along a shortest path are the body part positions that most closely fit the estimated lengths of the body. We now build upon this method of 3D human motion tracking to begin characterizing clinical gait data related to multiple sclerosis, without the need for wearable sensors or markers. Specifically, we seek to automatically quantify clinically relevant lower body gait parameters emergent in the literature: stride length, stride width and walking velocity [14]–[16]. Furthermore, we propose a movement towards upper body gait characteristics by implementing a measure of arm swing.

II. Methodology

We used a single depth sensing camera to record the motion of a walking person. The camera recorded 640x480 images at ~30 frames per second. We identify potential body part positions using the methods found in [5], then select accurate positions from these data using our optimization algorithm [13]. The selection of positions from multiple options can be seen in Fig. 1. These optimum selections serve as the initial part positions. To further improve the positions, we implement an algorithm that models a physical spring system, to move positions until they conform to a set of pre-estimated body lengths. We then calculate the following gait characteristics: walking velocity, stride length, stride width, and arm swing angle.

A. Spring System

After selecting optimal body positions from a set of options, the positions are further revised using the principle of energy minimization. The body parts on one quadrant of the body (e.g., lower left), act as the masses in a series of linear springs. There is one spring between each adjacent body part in a quadrant. The true lengths of the body links have been already estimated [13]. The resting length of a spring between two parts is set to be the estimated length of that link. Therefore, if the part positions are spaced too close or too far, the spring system will have potential energy. As the system reaches equilibrium, the part positions are moved to closely match the estimated body lengths.

The process is executed on each body quadrant (upper/lower, left/right), for each image frame. To ensure real-time processing, we use a method of fast spring simulation, which was developed for 3D computer graphics [17].

B. Gait parameters

1) Walking velocity: The velocity of the walking person is determined using the average position of the lower body parts and the head. The velocity vector $\mathbf{v}$ is defined as the difference between the current average position $\mathbf{P_{avg}}$, and the average position from the preceding image frame. As a clinical measure, we calculate the median and mean velocities over the image sequence.

2) Stride Length: Stride, as a clinical measure, has been referred to as a full gait cycle (two steps) [18], and to a half gait cycle [19]. We define the stride length SL as the distance between the two feet when the legs are apart, as in [19].

The left foot position $\mathbf{P_{lf}}$ and right foot position $\mathbf{P_{rf}}$ are estimated by our motion tracker. The absolute distance between the feet is calculated as

$$d_{feet} = ||\mathbf{P_{lf}} - \mathbf{P_{rf}}|| \tag{1}$$

During normal walking motion, the value of d_{feet} is periodic. The peaks occur when a person is in mid-stride. The stride length, as defined by [19] is the value of these peaks. Since our motion tracking can contain stochastic noise, there may be peaks of d_{feet} that are invalid. These outliers are dealt with by removing values that are beyond two standard deviations from the mean. The periodic nature of the motion makes it appropriate for curve fitting. Accordingly, we fit a sine wave to d_{feet} using the method of least squares.

3) Stride Width: While the stride length is calculated over a time duration, the stride width is calculated for each frame. First, the average three-dimensional position of the two feet is found, and its velocity vector is calculated by subtracting the previous position from the current. To smooth out the list of velocity vectors, the vector at the current frame is set to be the median of the vectors from the past 30 frames (equivalent to one second of time).

We define the stride width as the current distance between the two feet, in a direction perpendicular to the current velocity vector of the average position between the feet. The plane Π passes through the average position of the feet, and it is normal to the velocity vector of this average position. Both foot positions $\mathbf{P_{lf}}$ and $\mathbf{P_{rf}}$ are projected onto Π. The stride width SW is defined to be the distance between these projected points.

$$SW = ||\operatorname{proj}_{\mathbf{\Pi}} \mathbf{P_{lf}} - \operatorname{proj}_{\mathbf{\Pi}} \mathbf{P_{rf}}|| \tag{2}$$

4) Arm swing angle: The tracked upper body parts consist of the head, arm (approximately elbow), and hand. The vector from the head to the hand is recorded on each frame. The arm swing angle θ is calculated between this vector, and the reference vector $\hat{\jmath}$.

$$\theta = \cos^{-1}\left[(\mathbf{P_{head}} - \mathbf{P_{hand}}) \cdot \hat{\jmath}\right] \tag{3}$$

During a normal walking motion, the angle of this vector will be periodic, as the arm swings. The vector angle completes a period over a full swing cycle.

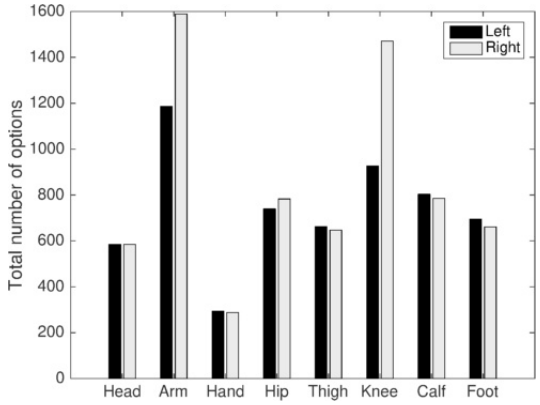

Figure 2. Total number of options (nodes in graph) for the body parts, across all image frames

III. Results

A total of 668 image frames were recorded. Of these, 279 had at least one predicted body part position. After implementing our method to select body part positions from multiple stochastic options [13], we use our spring system method to optimize these positions. We then calculate the key gait characteristics that can be used for clinical analysis. The entire image sequence was processed offline. The full process, including the pre-estimation of the body lengths, required 4.4 seconds, using a 2.9 GHz Intel Core i7 processor. Accordingly, this approach executes at 15.8 ms per frame of data, or approximately 63 fps.

On each image frame, four graphs were created, for the left/right sides, and the upper/lower body parts. The number of nodes in each graph varies between frames and parts. Fig. 2 shows the total number of nodes for each body part, which represent the optional part positions. The arm and knee had the greatest number of options available overall. The graph optimization process is a fast portion of the computation, requiring 2.6 ms per frame of data.

A. Spring System

On a given image frame, the actual body lengths (distances between adjacent body parts) may differ from the

Table I
WALKING SPEED STATISTICS [CM/S]

Mean	Median	Standard Deviation
151.4	136.0	76.7

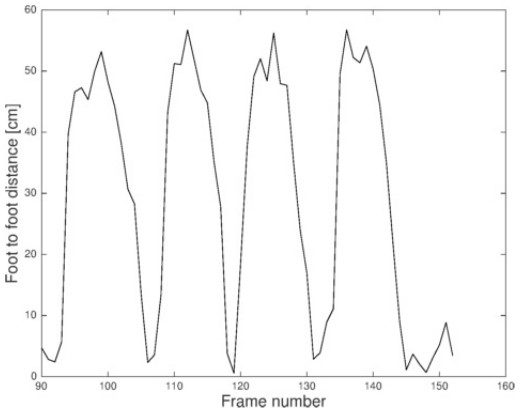

Figure 3. Distance between feet over a portion of the image frames

Table II
STRIDE WIDTH STATISTICS [CM]

Mean	Median	Standard Deviation
23.5	27.9	16.8

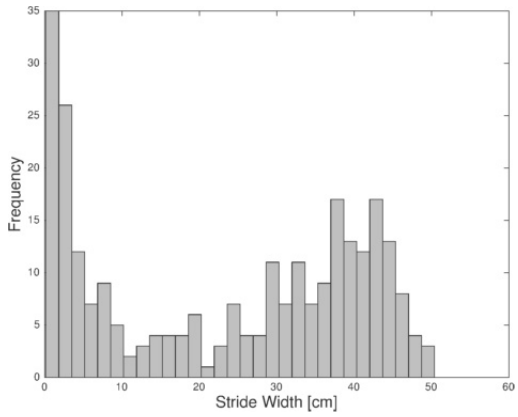

Figure 4. Histogram of stride width values, over the full data set

pre-estimated body lengths. The goal of the spring system is to adjust position predictions to match the pre-estimated body lengths, while minimizing the amount that the positions move. To evaluate the effect of the spring system, a cost was calculated between the estimated body lengths and the actual body lengths, on each image frame. The cost C between the estimated length vector L_{est} and the actual length vector L_{act} is

$$C = \sum_{i=0}^{N} ||L_{est,i} - L_{act,i}|| \tag{4}$$

where N is the number of lengths in both vectors. The average cost is the sum of each image cost C, divided by the total number of image frames. For the upper body, the average cost was originally 18.42 cm. After implementing the spring system, this was reduced to 3.05 cm. Similarly, for the lower body, the average cost dropped from 24.5 cm to 4.59 cm. The spring system is a relatively slow portion of the computation, requiring 7.4 ms per frame, or 46.8% of the total time.

B. Gait parameters

1) Walking velocity: The results for the magnitude of the walking velocity are shown in Table I. The median walking speed was found to be 1.36 m/s, which is within the range of normal average walking speed (1.25 - 1.5 m/s) [20].

2) Stride Length: The distance between feet varies in a periodic cycle as a person walks. Fig. 3 shows this distance plotted over 70 image frames. The peaks in the plot represent the instances when the person is in mid-stride. In order to analyze the stride length, a sine wave was fit to the data using the method of least squares. The data shown in Fig. 3 has a sine wave approximation of

$$y = 28.2\sin(0.46(x+1)) + 28.7 \tag{5}$$

where x is in radians. The stride length can be approximated by the maximum value of the sinusoidal wave, which is 56.9 cm. This approximation can also be used to determine the frequency of a walking cycle. The angular frequency ω is 0.46 rad/frame. As $\omega = 2\pi f$, the frequency is 0.073 cycles per frame. Given ~30 frames per second, the frequency is 2.20 cycles per second. As the person travels a full stride length over one cycle, their speed is $f \times SL = 125.0$ cm/s, which is acceptably close to the walking speed found in section III-B1.

After removing data points beyond two standard deviations from the mean, the maximum value of the full foot distance data set was found to be 56.75 cm, which is close to the sine wave approximation.

3) Stride Width: The mean, median, and standard deviation of the stride width are shown in Table II. There is a large degree of variability in the stride width values, as evidenced by the relatively large standard deviation, and as seen in Fig. 4.

4) Arm swing angle: The angle between the head and the hand is shown in Fig. 5 as a histogram for the left and right sides. The left arm is rotated by small angles more frequently than the right.

IV. DISCUSSION

The results from the spring process show that it is effective in moving the body part positions so that they better conform to the pre-estimated lengths between adjacent parts. While these results are positive, we have yet to determine that the inclusion of this process increases the overall accuracy of the positions. Ground truth measures will be needed to directly evaluate the benefit of including this function. Although nearly half of the computation time is devoted to the spring process, real time image processing is maintained.

The stride length was calculated by taking the maximum of the full data set, after removing outliers. It was also calculated by fitting a sine wave to a portion of the foot distance data, and taking the maximum value of this curve. The results from the two methods were very similar. The sine wave method had

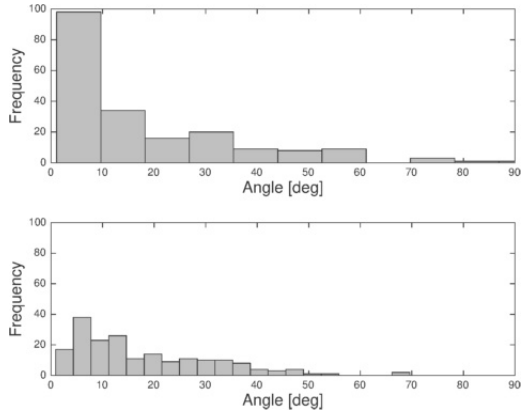

Figure 5. Histogram of head to hand angle for left arm (top) and right arm (bottom)

the added benefit of also calculating stride frequency, which can be used to determine walking speed. A composite of the two methods could involve removing outliers from the full data set, then fitting a sine wave to the entire set.

The accuracy of the stride width calculation is dependent on projecting the foot positions onto the correct plane. A plane is fully defined by its normal vector and a point on the plane. To ensure that the plane is always located between the feet, the point on the plane was chosen to be the average position of the feet. The stride width is intended to measure the foot to foot distance that is perpendicular to the direction of walking motion. Thus, the velocity vector of the average foot position was used. However, the average position of the feet could move in a direction other than the true direction of motion, from one frame to the next. To account for this, the median velocity of the past 30 frames was used, with the intention of capturing the true velocity direction of the person.

For clinical analysis, it may be useful to compare gait parameters from the left and right sides, which can be asymmetric [21]. The results for the arm angles demonstrate an asymmetry between the left and right arms, as there is a different frequency distribution of the angles (Fig. 5). The same method could be used for legs as well. The asymmetry between left and right sides of the body can be an indicator of abnormal gait, such as a limping motion.

V. Limitations and Future Work

The success of this system is based on two main areas: the accuracy of the motion tracking, and the calculation of gait metrics from the tracking data. Currently, the motion tracking algorithm has been optimized for a walking motion, and it may experience a reduction in accuracy when the walking is abnormal (e.g., stumbling, shuffling). Because this system is intended to be used for clinical gait analysis, it must be made robust to these types of motion, as they are more common among participants with progressed multiple sclerosis. In future work, gait metrics should be calculated using ground truth (e.g., manually annotated) motion tracking data, or to clinical ground truth evaluations, to remove the uncertainty introduced by our motion tracking. These gait metrics could then be compared to the metrics calculated using our motion tracking data.

If the accuracy of our system is found to be comparable to gold standard assessments, our methods may offer an inexpensive and portable method of unobtrusively obtaining clinical gait data. To further increase the potential relevance of our system, we will further investigate the types of gait measurements that are useful to multiple sclerosis clinicians, and attempt to obtain them using our system.

VI. Conclusion

We have presented a method of extracting clinically relevant gait metrics of persons with multiple sclerosis using a single, inexpensive depth sensor without wearable markers or sensors. The methods proposed can be easily extended to multiple depth sensors, which may be used to increase the accuracy of motion tracking and the range of physical coverage of the system. Our motion tracking is based upon producing stochastic options for human body parts in an image, and selecting from these options using graph theory principles. We have also made use of a simulation algorithm from computer graphics to further improve our predicted body part positions. Using these optimized motion tracking data, we employ statistical methods to calculate gait characteristics, including stride length and width, walking velocity and arm swing angle. The long term goal of this research is a system that is accurate, affordable, and portable, so it can become a viable alternative to other assessment equipment, while still providing objective information that can help understand disease progression in persons with multiple sclerosis.

References

[1] D. Hodgins, "The importance of measuring human gait," *Medical Device Technology*, vol. 19, no. 5, 2008.

[2] M. J. Socie, R. W. Motl, J. H. Pula, B. M. Sandroff, and J. J. Sosnoff, "Gait variability and disability in multiple sclerosis," *Gait and Posture*, vol. 38, no. 1, pp. 51–55, 2013.

[3] M. J. Socie and J. J. Sosnoff, "Gait variability and multiple sclerosis," *Multiple Sclerosis International*, vol. 7, 2013.

[4] R. W. Motl, M. D. Goldman, and R. Benedict, "Walking impairment in patients with multiple sclerosis: exercise training as a treatment option," *Neuropsychiatr Dis Treat*, vol. 6, pp. 767–774, 2010.

[5] S. Czarnuch and M. Ploughman, "Automated gait analysis in people with multiple sclerosis using two unreferenced depth imaging sensors: Preliminary steps," in *Newfoundland Electrical and Computer Engineering Conference*, 2014.

[6] "Zeno walkway," 2014. [Online]. Available: http://www.protokinetics.com/zenowalkway.html

[7] C. Prakash, A. Mittal, R. Kumar, and N. Mittal, "Identification of spatio-temporal and kinematics parameters for 2-d optical gait analysis system using passive markers," in *Computer Engineering and Applications (ICACEA), 2015 International Conference on Advances in*. IEEE, 2015, pp. 143–149.

[8] M. Gabel, R. Gilad-Bachrach, E. Renshaw, and A. Schuster, "Full body gait analysis with kinect," in *2012 Annual International Conference of the IEEE Engineering in Medicine and Biology Society*. IEEE, 2012, pp. 1964–1967.

[9] A. Nandy and P. Chakraborty, "A new paradigm of human gait analysis with kinect," in *Contemporary Computing (IC3), 2015 Eighth International Conference on*. IEEE, 2015, pp. 443–448.

[10] D. Leightley, M. H. Yap, and J. McPhee, "Automated analysis and quantification of human mobility using a depth sensor," 2016.

[11] I. H. López-Nava, I. González, A. Muñoz-Meléndez, and J. Bravo, "Comparison of a vision-based system and a wearable inertial-based system for a quantitative analysis and calculation of spatio-temporal parameters," in *Ambient Intelligence for Health*. Springer, 2015, pp. 116–122.

[12] S. Czarnuch and M. Ploughman, "Toward inexpensive, autonomous, and unobtrusive exercise therapy support for persons with ms," in *Americas Committee for Treatment and Research in Multiple Sclerosis*, 2016.
[13] A. Hynes and S. Czarnuch, "Combinatorial optimization for human body tracking," in *International Symposium on Visual Computing*. Springer, 2016 (Accepted).
[14] J. J. Sosnoff, B. M. Sandroff, and R. W. Motl, "Quantifying gait abnormalities in persons with multiple sclerosis with minimal disability," *Gait and Posture*, vol. 36, no. 1, pp. 154–156, 2012.
[15] U. Givon, G. Zeilig, and A. Achiron, "Gait analysis in multiple sclerosis: characterization of temporal-spatial parameters using gaitrite functional ambulation system," *Gait and Posture*, vol. 29, no. 1, pp. 138–142, 2009.
[16] C. L. Martin, B. A. Phillips, T. J. Kilpatrick, H. Butzkueven, N. Tubridy, E. McDonald, and M. P. Galea, "Gait and balance impairment in early multiple sclerosis in the absence of clinical disability," *Multiple Sclerosis*, vol. 12, no. 5, pp. 620–628, 2006.
[17] T. Liu, A. W. Bargteil, J. F. O'Brien, and L. Kavan, "Fast simulation of mass-spring systems," *ACM Transactions on Graphics (TOG)*, vol. 32, no. 6, p. 214, 2013.
[18] O. Blin, A.-M. Ferrandez, and G. Serratrice, "Quantitative analysis of gait in parkinson patients: increased variability of stride length," *Journal of the neurological sciences*, vol. 98, no. 1, pp. 91–97, 1990.
[19] H. Kunz and D. Kaufmann, "Biomechanical analysis of sprinting: decathletes versus champions." *British Journal of Sports Medicine*, vol. 15, no. 3, pp. 177–181, 1981.
[20] A. Segal, E. Rohr, M. Orendurff, J. Shofer, M. O'Brien, and B. Sangeorzan, "The effect of walking speed on peak plantar pressure," *Foot & Ankle International*, vol. 25, no. 12, pp. 926–933, 2004.
[21] W. Hoogkamer, S. M. Bruijn, and J. Duysens, "Stride length asymmetry in split-belt locomotion," *Gait & posture*, vol. 39, no. 1, pp. 652–654, 2014.